Available online at www.sciencedirect.com
ScienceDirect
Diamond & Related Materials 16 (2007) 725–729
DIAMOND AND RELATED MATERIALS
www.elsevier.com/locate/diamond

Growth of diamond nanocrystals by pulsed laser ablation of graphite in liquid

L. Yang [a], P.W. May [a,*], L. Yin [b], J.A. Smith [a], K.N. Rosser [a]

[a] School of Chemistry, University of Bristol, UK
[b] Department of Aerospace Engineering, University of Bristol, UK

Available online 18 December 2006

Abstract

Nanocrystalline diamond has been successfully synthesized at room temperature and pressure using the novel technique of pulsed laser ablation (Nd:YAG, 532 nm) of a graphite target in water. High-resolution transmission electron microscopy (HRTEM), selected area electron diffraction (SAED), and laser Raman spectroscopy have been used to characterise the nanocrystals and to confirm that they are diamond. Time-averaged optical emission spectroscopy showed the presence of H, C and O atoms in the ablation plume. Imaging of the light emitted from the plume showed that H atoms were formed in two regions, in the liquid above the graphite surface, and also in the air just above the water surface. The results are consistent with the idea that atomic H is a necessary requirement for the growth of diamond via this method.

Keywords: Diamond; Pulsed laser ablation; Nanoparticles; Nanodiamond

1. Introduction

Pulsed laser ablation (PLA) is a well-known technique to produce thin films by ablating material from a solid target of known composition [1]. PLA normally occurs in vacuum, or sometimes in an inert gas background, such as Ar, or in more reactive gases such as ammonia or nitrogen. A new variation of PLA has been reported recently whereby the target is immersed in a liquid medium, and the high-intensity laser beam is focused through the liquid onto the surface of the target [2,3]. In liquid phase PLA (LP-PLA), the interaction of the laser pulse with the target produces an ablation plume, in which the surface of the solid target and a small amount of the surrounding liquid are vaporised to form micro-bubbles within the liquid. The bubbles expand as more material is vaporised until, at a certain critical combination of pressure and temperature, they collapse [4]. It is believed that the species within the collapsing bubbles are subjected to temperatures of thousands of Kelvin and pressures of several GPa. These extreme conditions may allow novel materials to be created [4,5]. The conditions inside the bubbles are similar to the cavitation bubbles generated by ultrasonic waves or by arc discharges under liquids. Ionisation and breakdown of components within the bubbles can occur, and the subsequent electron-ion recombination followed by radiative cascade can produce significant optical emission. The advantage of LP-PLA is that large amounts of a solid target can be vaporised and incorporated into the bubble as well as the liquid, allowing compounds that contain a mixture of atoms from the target and the liquid to be made. Unlike the arc discharge method that requires the solid electrode material to be electrically conducting, LP-PLA can utilise insulating target materials, allowing a much wider range of novel materials to be produced. The products are usually in the form of nanoparticles that remain suspended within the liquid medium, and can be isolated by filtration and evaporation of the liquid.

This novel LP-PLA technique has been used to produce a variety of materials, including diamond-like carbon films from liquid aromatic hydrocarbons [6], nanocrystals of carbon nitride by ablating graphite in ammonia solution [7,8] and nanometre-sized particles of Ti, Ag, Au, Si and TiC [9]. Recently, Wang et al. [10] converted hexagonal boron nitride crystals into cubic boron nitride crystals using this method. Nanocrystalline diamond has also been produced by LP-PLA using a graphite target along with water or acetone as the liquid medium [11,12]. The main conclusions achieved by these researchers were that OH groups formed from the oxygen-containing liquids were etching non-diamond carbon species from the surface, thereby allowing diamond to form preferentially. Thus, the OH was thought to be playing a role analogous to that of atomic

* Corresponding author. Tel.: +44 117 928 9927; fax: +44 117 925 1295.
E-mail address: paul.may@bris.ac.uk (P.W. May).

0925-9635/$ - see front matter © 2006 Elsevier B.V. All rights reserved.
doi:10.1016/j.diamond.2006.11.010

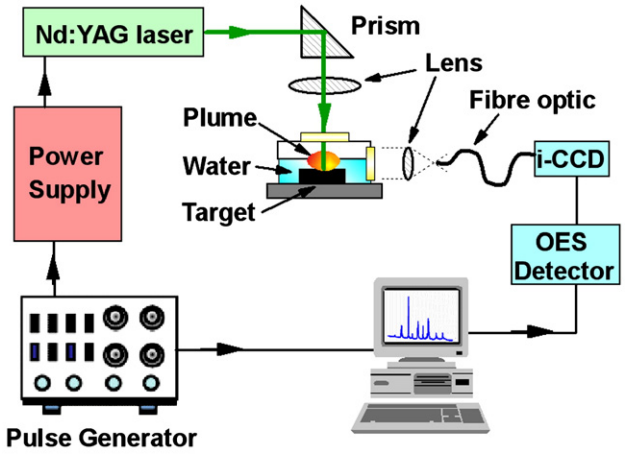

Fig. 1. Experimental setup for LP-PLA and optical emission spectroscopy.

hydrogen in conventional diamond CVD [13]. However, we recently showed [14] that diamond particles could be made using LP-PLA in cyclohexane, suggesting that OH is not necessary for diamond formation.

Although LP-PLA is becoming established as a route to diamond nanoparticle synthesis, a detailed description of the fundamental processes occurring in the laser–solid–liquid system is still lacking. To this end, in this paper we shall present results about LP-PLA nanocrystal diamond growth from graphite/water, together with a study of the optical emission from the plume.

2. Experimental details

The ablation apparatus (Fig. 1) consisted of two types of reaction cell, containing a graphite target (Testbourne Ltd., 99.99%) and 5–10 ml of deionised water, which covered the target to depth of 5 mm. The first type of cell was a simple open container, which allowed the ablation plume to be viewed easily for optical emission experiments. However, this cell had the disadvantage that the water could splash out from the cell at every laser pulse, requiring the liquid level to be constantly topped-up. The second type was a sealed stainless steel cell, which prevented the splashing but had less access for spectroscopic measurements.

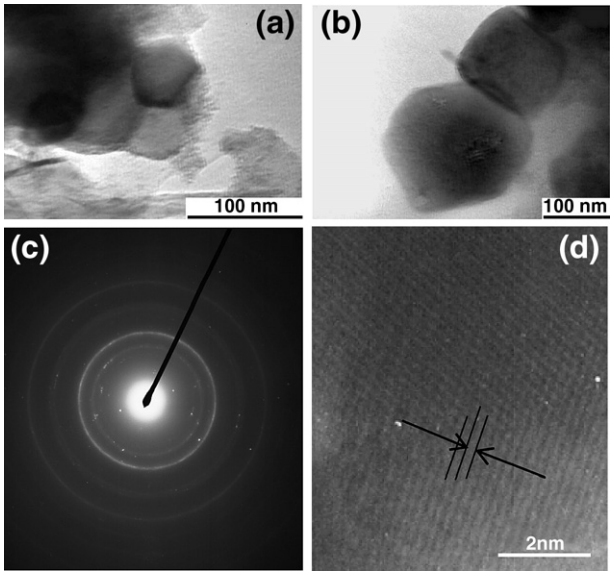

Fig. 2. TEM images of samples produced by pulsed laser ablation of a graphite target in water (laser fluence at 125 mJ per pulse) for durations of: (a) $t=0.5$ h, (b) $t=1$ h. (c) A typical SAED pattern taken from (a). (d) HRTEM lattice planes corresponding to diamond (111) planes.

Table 1
The lattice d-spacings of the four inner rings calculated from the SAED data (Fig. 1(c)) with comparison to those for diamond and graphite [19,20]

$d_{experiment}$/Å	$\langle hkl\rangle_{diamond}$	$d_{diamond}$/Å	$d_{graphite}$/Å
2.534	<110>	2.522	3.355
2.034	<111>	2.059	2.034
1.283	<220>	1.261	1.232
1.186	<300>	1.189	1.157

The incident beam was the second harmonic of a Nd:YAG laser (Spectron Laser System, 532 nm) which was directed by a prism and then focused using a 50 mm-focal-length biconvex lens through the liquid layer and onto the surface of the target to produce a spot size of ~0.5 mm diameter. The laser output had a pulse length of 15 ns and energy of approximately 125 mJ per pulse, which is sufficient to easily obtain breakdown in water. The laser fluence at the target surface was ~28 J cm^{-2}. The ablation was performed for times of 0.5–1 h.

After irradiation, the liquid often appeared slightly coloured (usually pale yellow) due to the suspension of nanoparticles. This suspension was pipetted onto microscope slide or transmission electron microscope (TEM) grids. The TEM grids (Agar Scientific) were SiO_2-coated to ensure that the elemental fingerprint of the sample was not confused with that from the grid. TEM and selected area electron diffraction (SAED) using a JEOL-1200 microscope, high resolution (HR) TEM (JEOL 2010 microscope) with energy dispersive X-ray (EDX) analysis were employed to identify the compositional, structural and morphology information of the prepared materials. Laser Raman spectroscopy (Renishaw 2000, excitation wavelength 325 nm) was used to study the bonding configuration.

Optical emission accompanying the LP-PLA process was viewed through a quartz window on the side of the cell, perpendicular to the laser direction (see Fig. 1). The emission was focused onto the entrance of a translatable single quartz fibre, the exit of which was adjacent to the entrance slit of a 0.32 m spectrometer. A narrow band-pass interference filter was placed in front of the camera to block out the scattered light from the laser beam between 515–545 nm, but allows other wavelengths to pass through to the detector. Since the duration of the laser pulse and the emission lifetimes of the species within the plume were much shorter than the minimum exposure time for the detector (~0.019 s), it was not possible to record a series of time-resolved spectra showing the evolution of the emitting region. Therefore, the spectra were captured using a 1 μs time gate, delayed by 120 ns from the start of the laser excitation, and accumulated over 100 laser shots. This gave a time-averaged total emission spectrum covering the period of the whole ablation process.

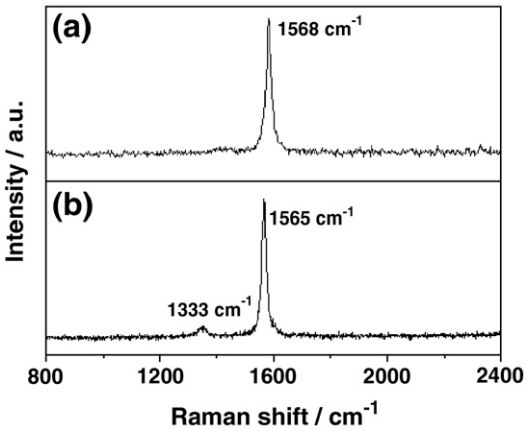

Fig. 3. Raman spectra of (a) the graphite target and (b) the nanocrystals formed by LP-PLA of graphite in water at 125 mJ laser fluence and 1 h ablation time.

Side-view images of the surface plasma emission were obtained by using an intensified charge-coupled device (i-CCD) connected to a computer with video capture software. The images were recorded by taking a continuous video during several laser pulses and analysing each frame of the video. A 656 nm filter (corresponding to the H Balmer emission line) was placed in front of the camera in order to obtain spatial information about the H atoms within the plume.

3. Results and discussion

The TEM analysis revealed that the ablated product contained a mixture of amorphous carbon and graphite from the target, plus a small amount of faceted crystalline nanostructures. EDX spectra indicated the presence of only C, Si and O in the area being studied (Si and O were from the TEM grid). Fig. 2(a) shows some typical facetted nanocrystals which were found at the edges of larger pieces of graphite, following 30 min ablation of graphite in water. The size of the crystallites (Fig. 2(b)) increased to ~100 nm when the reaction time doubled to 1 h. Similar morphology for diamond crystals is commonly seen in gas-phase CVD deposition [15,16]. A typical SAED ring pattern from the nanocrystals is shown in Fig. 2(c), and the lattice plane spacings for the four inner rings were analysed using a standard computer program [17]. They corresponded well to the {110}, {111}, {220} and {300} planes of diamond [19,20], as can be seen in Table 1. The observed lattice planes (Fig. 2(d)) in HRTEM are consistent with the (111) planes of crystalline diamond with an interplanar distance of 2.06 Å [18]. The above analyses are all consistent with a hexagonal diamond structure, similar to that reported in Refs. [19,20].

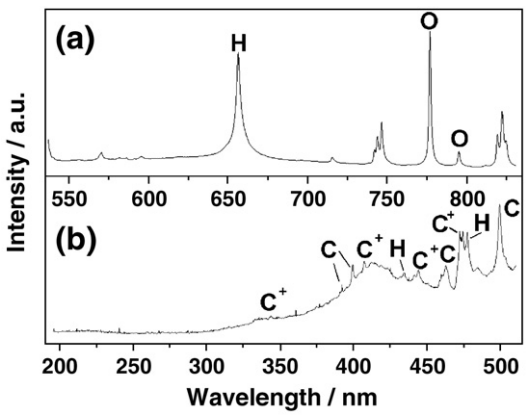

Fig. 4. Wavelength-dispersed optical emission spectra of the plume accompanying 532 nm LP-PLA of graphite in water. The spectrum has been split into two halves, (a) and (b), either side of the intense reflected laser peak at 532 nm (not shown). The features have been assigned to atomic H, O, and C, and C^+ ions (using literature values [22,23] as reference). The features around 740 and 825 nm have not been assigned but are possibly due to N_2.

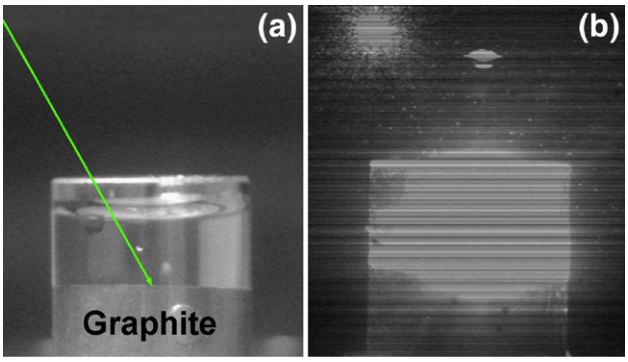

Fig. 5. (a) Photograph of the open cell showing the position of water and graphite target, as well as the direction of the laser beam (directed at an oblique angle to try to reduce the chance of water splashing onto the prism). (b) Image immediately following the laser pulse, showing the bright emission from the ablation plume. Top left shows emission from a droplet which has passed directly through the laser beam and scattered/re-emitted light.

The Raman spectra of the (a) target graphite bulk and (b) nanocrystals are shown in Fig. 3. After laser irradiation, the

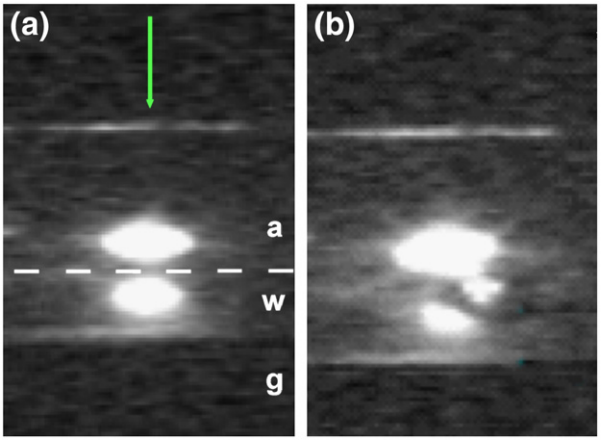

Fig. 6. Two i-CCD images of the total emission resulting from 532 nm, 15 ns PLA of graphite in water recorded using an H Balmer (656 nm) filter in front of the camera. The white dashed line shown in (a) indicates the position of the interface between the water, w, and air, a, with graphite target, g, below. The bright horizontal line near the top of each image is the top edge of the cell window through which the laser (illustrated by the arrow) passes. Each laser pulse produced a slightly different image, of which most resembled (a) with bright plasma balls in both the water and the air directly above the surface of the target. However, sometimes the images showed secondary plasma balls, such as in (b), probably due to the ejection of larger graphitic particulates from the target interacting with and being excited by the laser pulse.

spectrum from the graphite target shows only the G band at 1568 cm^{-1} arising from ordered graphite [21]. The Raman spectrum from the nanoparticles also showed the G band (but with a slight shift to 1565 cm^{-1}) which could indicate the presence of bond-angle disorder. A weak peak at 1333 cm^{-1} is also seen as the fingerprint for sp^3-bonded C in diamond [21]. The relative size of the G band to that of the diamond peak is not unexpected given the low yield of diamond nanoparticles in the graphite background.

Fig. 4 shows wavelength-resolved emission spectra of the ablation plume induced by 532 nm laser excitation. Emission from atomic C and C^+ is observed as a direct result of the ablation process. But the presence of atomic H and O shows that the water is also being dissociated in the PLA process, either directly by interaction with the high energy laser, or indirectly as a result of reactions with the high kinetic energy ejected atoms and particles in the plume. Such plume reactions have been seen previously during PLA of graphite in vacuum or in gaseous nitrogen or argon, backgrounds [22–24]. The presence of the strong peaks from atomic H is interesting, since H is believed to be necessary for the growth of diamond in conventional gas-phase CVD methods [13]. Peaks from atomic H were also seen previously during diamond growth from LP-PLA of graphite in cyclohexane [14]. This suggests that atomic H may be a common reagent necessary in both LP-PLA and CVD diamond growth, and that the growth mechanism may therefore be similar in both systems.

Fig. 5 shows an example image of the ablation plume at the graphite–water interface following frame-capture by a video camera. Fig. 5(a) shows the geometry of the open cell before the laser pulse occurs. Fig. 5(b) is an example of one of the emission plumes seen during ablation. There were considerable shot-to-shot variations in the shape and size of the emission, resulting from non-uniformities in the target surface, bubbles within the liquid, and droplets ejected into the air. In Fig. 5(b), numerous small droplets can be seen being ejected from the cell, one of which (top left) has passed directly through the laser beam and scattered/re-emitted light.

Fig. 6 shows two typical frame images captured from the video when using a 656 nm filter to observe only the emission from atomic H. It can be seen in Fig. 6(a) that the H emission arises from two regions along the path of the laser pulse, one within the water close to the target, and the other in the air a few mm above the water surface. This suggests that the time-averaged emission shown previously (Fig. 5) is actually a result of at least two separate processes. In the water region, excited H atoms are being created either as a result of (i) direct laser interaction causing breakdown of the water, or (ii) reaction between water and energetic ablated C atoms, ions or particles ejected from the surface, or (iii) the collapse of cavitation bubbles [4]. The presence of atomic H in the liquid phase near to the graphite surface is consistent with the idea that H is required for graphite-to-diamond conversion. Excited H atoms are also created in the air region, again as a result of processes (i) or (ii). Fig. 6(b) shows another captured image displaying a smaller secondary emission region within the water. These secondary plasma regions sometimes occurred within the liquid, or in the air, or in both simultaneously, and highlight the shot-to-shot variability of the process.

4. Conclusions

We have demonstrated that nanocrystalline diamond particles can be formed using LP-PLA. TEM/SAED/Raman analyses confirm that the ablated material is consistent with a faceted diamond phase. Optical emission spectroscopy shows that the ablation process produces two plasma regions, one confined into the liquid and one in the air just above the liquid surface. Emission from atomic H within these regions is consistent with the idea that H is required for diamond growth, even in an aqueous medium. To gain further insight into this mechanism, an obvious extension of this work would be to perform time resolved studies using a fast gated CCD, and to increase the spatial resolution so that the emission from the air and water regions could be imaged separately.

However, from analysis of the composition of the ablation product, we estimate that the yield of nanodiamond particles is only about 5%, with the remainder being graphitic particles ejected from the target. Thus, development of a suitable separation procedure would be required to increase the efficiency of this process, and this would essential if LP-PLA were to be used as a commercially viable method of producing nanodiamond. Possible routes might be oxidation and removal of the unwanted graphitic particles using hot, strong acids, and/or separation methods using high-speed centrifuge followed by filtration techniques.

Acknowledgements

The authors are grateful to the University of Bristol for financial support of this work via a Research Scholarship, and to the Overseas Research Scholarship (ORS) scheme for a post-graduate scholarship (Li Yang), and to S.A. Davis, J. Jones, and C. Archer for their many and varied contributions to the work described herein.

References

[1] P.R. Willmott, J.R. Huber, Rev. Mod. Phys. 72 (2000) 315.
[2] P.P. Patil, D.M. Phase, S.A. Kulkarni, S.V. Ghaisas, S.K. Kulkarni, S.M. Kanrtkar, S.B. Ogale, V.G. Bhide, Phys. Rev. Lett. 58 (1987) 238.
[3] J. Singh, M. Vellaikal, J. Narayan, J. Appl. Phys. 73 (1993) 4351.
[4] O. Yavas, A. Schilling, J. Bischof, J. Boneberg, P. Leiderer, Appl. Phys., A Mater. Sci. Process. 64 (1997) 331.
[5] S.J. Shaw, W.P. Schiffers, T.P. Gentry, D.C. Emmony, J. Phys., D, Appl. Phys. 32 (1999) 1612.
[6] A.V. Simakin, V.V. Voronov, N.A. Kirichenko, G.A. Shafeev, Appl. Phys., A 79 (2004) 1127.
[7] G.W. Yang, J.B. Wang, Appl. Phys., A Mater. Sci. Process. 71 (2000) 343.
[8] L. Yang, P.W. May, L. Yin, R. Brown, T. Scott, Chem. Maters 18 (2006) 5058.
[9] S.S.I. Dolgaev, A.V. Simakin, V.V. Voronov, G.A. Shafeev, Appl. Surf. Sci. 186 (2002) 546.
[10] J.B. Wang, G.W. Yang, C.Y. Zhang, X.L. Zhong, Z.H.A. Ren, Chem. Phys. Lett. 367 (2003) 10.
[11] J.B. Wang, C.Y. Zhang, X.L. Zhong, G.W. Yang, Chem. Phys. Lett. 361 (2002) 86.
[12] J.B. Wang, G.W. Yang, J. Phys., Condens. Matter 11 (1999) 7089.
[13] P.W. May, Philos. Trans. R. Soc. Lond., A 358 (2000) 473.
[14] S.R.J. Pearce, S.J. Henley, F. Claeyssens, P.W. May, K.R. Hallam, J.A. Smith, K.N. Rosser, Diamond Relat. Mater. 13 (2004) 661.
[15] M.N.R. Ashfold, P.W. May, C.A. Rego, N.M. Everitt, Chem. Soc. Rev. 23 (1994) 21.

[16] P.G. Partridge, M.N.R. Ashfold, P.W. May, E.D. Nicholson, J. Mater. Sci. 30 (1995) 3973.
[17] J.L. Lábár, in: L. Frank, F. Ciampor (Eds.), Proceedings of EUREM, vol. III, 12, July 2000, p. I379, Brno.
[18] A.L. Vereshchagin, G.S. Yur'ev, Inorg. Mater. 39 (2003) 247.
[19] G.W. Yang, J.B. Wang, Q.X. Liu, J. Phys., Condens. Matter 10 (1998) 7923.
[20] T. Yagi, W. Utsumi, M. Yamakata, T. Kikegawa, O. Shimomura, Phys. Rev., B 46 (1992) 6031.
[21] J. Filik, Spectrosc. Eur. 17 (2005) 10.
[22] F. Claeyssens, M.N.R. Ashfold, E. Sofoulakis, C.G. Ristoscu, D. Anglos, C. Fotakis, J. Appl. Phys. 91 (2002) 6162.
[23] G.M. Fuge, M.N.R. Ashfold, S.J. Henley, J. Appl. Phys. 99 (2006) 014309.
[24] G.M. Fuge, C.J. Rennick, S.R.J. Pearce, S.J. Henley, P.W. May, M.N.R. Ashfold, Diamond Relat. Mater. 12 (2003) 1049.